HHS Public Access

Author manuscript

J Cell Physiol. Author manuscript; available in PMC 2024 June 01.

Published in final edited form as:

J Cell Physiol. 2023 June ; 238(6): 1368–1380. doi:10.1002/jcp.31014.

Decreased CRISPLD2 expression impairs osteogenic differentiation of human mesenchymal stem cells during *in vitro* expansion

Weiqiong Rong[1], **Calvin P. Rome**[1], **Marilyn A. Dietrich**[2], **Shaomian Yao**[1]

[1] Department of Comparative Biomedical Sciences, School of Veterinary Medicine, Louisiana State University, Baton Rouge, LA 70803, USA

[2] Department of Pathobiological Sciences, School of Veterinary Medicine, Louisiana State University, Baton Rouge, LA 70803, USA

Abstract

Human mesenchymal stem cells (hMSCs) are the cornerstone of regenerative medicine; large quantities of hMSCs are required via *in vitro* expansion to meet therapeutic purposes. However, hMSCs quickly lose their osteogenic differentiation potential during *in vitro* expansion, which is a major roadblock to their clinical applications. In this study, we found that the osteogenic differentiation potential of human bone marrow stem cells (hBMSCs), dental pulp stem cells (hDPSCs), and adipose stem cells (hASCs) was severely impaired after *in vitro* expansion. To clarify the molecular mechanism underlying this *in vitro* expansion-related loss of osteogenic capacity in hMSCs, the transcriptome changes following *in vitro* expansion of these hMSCs were compared. Cysteine-rich secretory protein LCCL domain-containing 2 (CRISPLD2) was identified as the most downregulated gene shared by late passage hBMSCs, hDPSCs, and hASCs. Both the secreted and non-secreted CRISPLD2 proteins progressively declined in hMSCs during *in vitro* expansion when the cells gradually lost their osteogenic potential. We thus hypothesized that the expression of CRISPLD2 is critical for hMSCs to maintain their osteogenic differentiation potential during *in vitro* expansion. Our studies showed that the knockdown of CRISPLD2 in early passage hBMSCs inhibited the cells' osteogenic differentiation in a siRNA dose-dependent manner. Transcriptome analysis and immunoblotting indicated that the CRISPLD2 knockdown-induced osteogenesis suppression might be attributed to the downregulation of matrix metallopeptidase 1 (MMP1) and forkhead box Q1 (FOXQ1).

Address for correspondence: Shaomian Yao, Department of Comparative Biomedical Sciences, School of Veterinary Medicine, Louisiana State University, Baton Rouge, LA 70803, USA, shaomia@lsu.edu.

Author contributions

Weiqiong Rong designed and performed experiments, analyzed data, wrote the manuscript; Calvin P. Rome performed experiments, analyzed data, and reviewed the manuscript; Marilyn A. Dietrich conducted FACS experiment, collected the data, and reviewed the manuscript; Shaomian Yao conceived the research, designed and performed experiments, analyzed data, edited the manuscript, and supervised the study.

Conflict of interest

The authors declare no conflict of interest.

Ethics approval statement

All human cell handling protocols were approved by the Louisiana State University/Louisiana Agriculture Center Inter-Institutional Biological and Recombinant DNA Safety Committee (IBRDSC). The use of the human stem cells for research was also approved by the Institutional Review Board of Louisiana State University.

Furthermore, adeno-associated virus (AAV)-mediated CRISPLD2 overexpression could somewhat rescue the impaired osteogenic differentiation of hBMSCs during *in vitro* expansion. These results revealed that the downregulation of CRISPLD2 contributes to the impaired osteogenic differentiation of hMSCs during *in vitro* expansion. Our findings shed light on understanding the loss of osteogenic differentiation in hMSCs and provide a potential therapeutic target gene for bone-related diseases.

Keywords

CRISPLD2; osteogenic differentiation; hBMSCs; hDPSCs; hASCs

Introduction

Human mesenchymal stem cells (hMSCs) are adult stem cells that could be isolated from multiple tissues such as bone marrow (hBMSCs), dental pulp (hDPSCs) and adipose (hASCs), etc. They can differentiate into various cell types, including osteoblasts, adipocytes and chondrocytes under appropriate conditions to participate in the tissue remodeling and repair (Pittenger et al., 1999). MSCs are promising cell sources for bone tissue regeneration, primarily owing to their superior osteogenic differentiation capacity. Long-term *in vitro* expansion of hMSCs is essential to scale up the cell quantities to meet the therapeutic cell dosage levels as MSCs are a rare population residing in human tissues. For example, in bone marrow aspirates, only 0.001–0.01% of the nucleated cells are hMSCs, but 10–400 million hMSCs are required for each cell therapy, which gives rise to 8–12 weeks' *in vitro* expansion of hMSCs before implantation (Kureel et al., 2019; Musiał-Wysocka et al., 2019; Ren et al., 2012; Wexler et al., 2003). However, hMSCs quickly lose their osteogenic differentiation potential during *in vitro* expansion, which largely hampers their clinical applications. It has been documented in the literature the reduction of differentiation capability in MSCs as early as the 1st or 2nd passage (Chen et al., 2005) with total loss of differentiation capability around the 6th passage (Bonab et al., 2006; Vacanti et al., 2005). Moreover, hBMSCs must be used at early passages for osteogenic differentiation due to the rapid loss of osteogenic capability (Yang et al., 2018). However, the molecular mechanisms underlying this phenomenon are largely unknown. To circumvent this limitation, it is of the utmost importance to understand the mechanisms of osteogenic regulation during *in vitro* expansion of hMSCs to facilitate the development of new cell expansion strategies for preserving their potential. Here, we report our findings to begin address this issue.

Cysteine-rich secretory protein LCCL domain-containing 2 (CRISPLD2), also known as late gestation lung 1 (LGL1), is a secreted glycoprotein that presents in lung, kidney, heart, liver, etc., and is well-conserved in mammals (Kaplan et al., 1999; Oyewumi et al., 2003b). Further characterization of CRISPLD2 suggests that it is secreted by mesenchymal cells to affect lung and kidney branching morphogenesis and lung alveologenesis (Nadeau et al., 2006; Oyewumi et al., 2003a; Oyewumi et al., 2003b; Quinlan et al., 2007). Homozygous CRISPLD2 knockout mice are embryonically lethal. Heterozygous CRISPLD2 knockout mice display aberrant lung formation, manifested by distal airspace enlargement, disorganized elastin fibers, and altered lung mechanics at maturity (Lan et

al., 2009). In addition to lung and kidney development, CRISPLD2 is also involved in the development of nonsyndromic cleft lip with or without cleft palate (Chiquet et al., 2007; Letra et al., 2011). Disruption of CRISPLD2 in zebrafish leads to craniofacial abnormalities through modulating the migration, differentiation, and/or survival of neural crest cells (Swindell et al., 2015; Yuan et al., 2012). It is shown that CRISPLD2 is significantly increased in mouse adipose tissue during weight loss, suggesting its role in adipocyte remodeling (Jackson et al., 2019). In hBMSCs, Brachtl et al. reported a strong positive correlation between CRISPLD2 expression and 3D chondrogenesis (Brachtl et al., 2022). Recently, single-cell sequencing revealed transcriptome changes over successive passages of hBMSCs during *in vitro* culture and identified CRISPLD2 as the top downregulated gene in late passage compared to early passage hBMSCs (Liu et al., 2019). Together, CRISPLD2 may mediate the regulation of hMSC differentiation during *in vitro* expansion.

In the present study, we first found that the gradually declined osteogenic differentiation potential during *in vitro* expansion of hBMSCs, hDPSCs, and hASCs is not due to the overgrowth of non-stem cells in the population but is concordant with the progressive downregulation of CRISPLD2. We further demonstrated that knockdown of CRISPLD2 inhibits osteogenic differentiation of hBMSCs in a siRNA dose-dependent manner. Furthermore, AAV-mediated CRISPLD2 overexpression could attenuate impaired osteogenesis of hBMSCs during *in vitro* expansion. Overall, our results indicated that decreased CRISPLD2 expression contributes to the loss of osteogenic capacity of hMSCs during *in vitro* expansion.

Materials and methods

Cell culture

The primary hBMSCs and hASCs were purchased from Obatala Sciences (New Orleans, LA, USA), and hDPSCs were purchased from Lonza. The cells were cultured in Minimum Essential Medium Alpha (MEM-α, Corning) containing 20% (v/v) fetal bovine serum (FBS, Neuromics) and 1% (v/v) penicillin-streptomycin (Gibco) in a humidified incubator infusing 5% CO_2 at 37°C with medium replacement every 3–4 days. Once the cells reached 90% confluency, TrypLE™ Express (Gibco) was used to detach the cells from cell culture flasks (CELLSTAR®, Greiner Bio-One), and the cells were then passaged at a 1:3 ratio to different passages until passage 11. Cells at each passage were pooled, centrifuged (300 × *g*, 5 min), and resuspended in the cell freezing medium consisting of 50% (v/v) MEM-α, 40% (v/v) FBS, and 10% (v/v) DMSO, followed by cryopreservation in liquid nitrogen. Passage 3 (P3) was referred to as the early passage, whereas passage 9 (P9) and passage 11 (P11) were late passages in this study. Cells at specific passage were recovered in designated culture devices depending on different experiments (i.e., T-75 flasks for cell expansion and fluorescence-activated cell sorting (FACS); T-25 flasks for RNA sequencing (RNA-seq) and western blot analysis; 6- or 12-well plates for gene expression analysis by quantitative real-time PCR (qRT-PCR); 24-well plates for alizarin red s (ARS) staining, and calcium quantification). AAV packaging cell line, AAVpro 293T cells, purchased from Takara Bio USA, Inc. (San Jose, CA, USA), were grown in Dulbecco's Modified Eagle's Medium (DMEM, GenClone, or ATCC) with 10% (v/v) FBS and 1% (v/v) penicillin-streptomycin.

Cells were maintained according to the manufacturer's guidelines. All human cell handling protocols were approved by the Louisiana State University/Louisiana Agriculture Center Inter-Institutional Biological and Recombinant DNA Safety Committee (IBRDSC). The use of the human stem cells for research was also approved by the Institutional Review Board of Louisiana State University.

Fluorescence-activated cell sorting (FACS)

hBMSCs, hDPSCs, and hASCs at passages 3, 5, 9, and 11 were detached from flasks when the cells grew to 90% confluency. The cells were collected and resuspended in 1 × DPBS with 1% (v/v) FBS (namely 1 × DPBSF) and filtered through 40 μm cell strainers to prepare a single-cell suspension. Next, the single-cell suspensions were incubated with APC-conjugated CD90 (BioLegend, cat. # 328114) and FITC-conjugated CD105 (BioLegend, cat. # 323204) antibodies at 1:20 dilution for 20 min on ice and 5 min at room temperature. After incubation, the cells were washed with 3 ml 1 × DPBSF to remove unbound antibodies. The supernatants were discarded following centrifugation at 300 × *g* for 5 min, and the cell pellets were resuspended in 1 × DPBSF at a cell density of 1×10^6 cells/100 μl and analyzed by a flow cytometer (FACS Aria II cell sorter, BD Biosciences).

Osteogenic induction, alizarin red s (ARS) staining and calcium quantification

hMSCs were cultured in osteogenic medium consisting of MEM-α medium, 10% (v/v) FBS, 0.5% (v/v) penicillin-streptomycin, and human osteogenic supplement (R&D Systems, Minneapolis, MN) when the cells were 80%–90% confluent. Osteogenic induction was achieved by maintaining the cells in the osteogenic medium for two or three weeks with medium change every 3–4 days.

ARS staining was used to visualize calcium deposits in cell culture, as described earlier (Rong et al., 2022). Briefly, cells were washed twice with 1 × PBS and fixed with 10% neutral buffered formalin (Sigma) for 5 min at room temperature. After washing with deionized water, the cells were stained with 1% ARS solution (GFS Chemicals, Columbus, OH, USA) for 5 min and rinsed with water to remove the excessive dye. The calcium deposits were observed under a microscope and imaged with an Olympus Q-Color3™ imaging system.

To quantify calcium deposition in osteogenic differentiated hMSCs, the cells were washed twice with 1 × DPBS followed by calcium collection with 250 μl/well (24-well plate) of 0.6 N HCl solution at 4°C for 2 days. The calcium concentration in the solution was then quantitated by a QuantiChrom™ Calcium Assay kit (BioAssay Systems, Hayward, CA, USA) according to the manufacturer's protocol.

Small interfering RNA (siRNA)-mediated CRISPLD2 knockdown

Dicer-substrate CRISPLD2 siRNA (siCRISPLD2) and scrambled siRNA negative control (siNC) were purchased from Integrated DNA Technologies (Coralville, IA, USA). The sequences were listed in Table S1. siCRISPLD2 or siNC was transfected into early passage hMSCs either in the growth medium or in the osteogenic medium at a final concentration of 20 and 40 nM (using Lipofectamine® RNAiMAX Reagent; Invitrogen)

or 25 nM (using TransIT-X2® Dynamic Delivery System; Mirus Bio, Madison, WI, USA) according to manufacturers' protocols. Briefly, siCRISPLD2 or siNC was prepared with transfection reagents in Opti-MEM® I Reduced-Serum Medium (Gibco) to allow the formation of liposome/polymer-siRNA complex, which was then added to cells dropwise. On day 3 post-transfection, the siRNA-containing medium was completely replaced with fresh growth/osteogenic medium. Transfection was repeated in the middle of 2–3 weeks' osteogenic induction to ensure continuous knockdown. CRISPLD2 knockdown efficiency was evaluated by qRT-PCR and western blot as detailed below.

Adeno-associated virus (AAV)-mediated CRISPLD2 overexpression

AAV serotype 2 (AAV2) particles overexpressing CRISPLD2 (AAV2-CRISPLD2) were produced by using AAVpro® Helper Free System (TaKaRa Bio Inc.) based on the manufacturer's instructions. Briefly, the human CRISPLD2 CDS region was cloned into pAAV-CMV vector, followed by DNA sequencing to verify the insertion (Table S2). The recombinant pAAV-CMV-CRISPLD2 vector was then co-transfected with pRC2-mi342 and pHelper vectors into AAVpro 293T cells at a 1:1:1 ratio with Lipofectamine® 3000 transfection kit (Thermo Fisher Scientific). The next day, the medium was replaced with fresh DMEM containing 2% (v/v) FBS. Three days post-transfection, the AAV2 particle-producing cells were collected for AAV2 isolation using the AAV extraction solution (TaKaRa Bio Inc.). The empty pAAV-CMV without CRISPLD2 insertion was packaged (AAV2-NULL) accordingly to serve as a negative control. The titer of AAV was determined by qRT-PCR with a published method (Aurnhammer et al., 2012; Gaj & Schaffer, 2016).

For transduction of hBMSCs, the cells were incubated in the growth medium containing a designated multiplicity of infection (MOI) of AAV when the cells reached 90% confluency. The infection medium was completely replaced with fresh culture medium the next day. After 3 and 7 days, the transduced cells were harvested to analyze CRISPLD2 expression either by qRT-PCR or western blot analysis as described below. To assess the effect of CRISPLD2 overexpression on osteogenic differentiation, the growth medium was replaced with osteogenic medium on day 3 post-transduction. After three weeks of osteogenic induction, the transduced cells were fixed and stained with ARS to show the calcium deposition.

Quantitative real-time PCR (qRT-PCR)

Cells were lysed in TRI Reagent (Molecular Research Center, Inc.) for total RNA extraction using either Direct-zol™ RNA kit (Zymo Research, Irvine, CA, USA) or the traditional method of bromochloropropane (BCP) separation and isopropanol precipitation, followed by Turbo™ DNase digestion to eliminate possible DNA contamination. The RNA quality and quantity were measured with a Nanodrop spectrometer at OD260 and 280. Samples with OD260/280 > 1.8 were used for RT-PCR analysis. Specifically, 500–1000 ng RNA was reverse-transcribed into cDNA with M-MLV reverse transcriptase (Invitrogen) following the manufacturer's protocol. cDNA was then mixed with iTaq Universal SYBR Green Supermix (Bio-Rad) and gene-specific primers (Table S3) and amplified on an ABI 7300 Real-Time PCR System (Applied Biosystems) to obtain CT values as described previously (Rong et al., 2022). The $2^{-\Delta\Delta ct}$ method was used to calculate the relative gene expression.

Western blot analysis

To determine the protein level of CRISPLD2, cells were harvested in cell lysis buffer (50 mM Tris-HCl (pH 7.5), 100 mM NaCl, 0.5% Triton-X-100, 5% glycerol) supplemented with protease inhibitor cocktail (Santa Cruz), then placed on ice for 15 min. The supernatants were collected after centrifugation at 13,000 rpm for 15 min at 4°C. Protein concentrations were quantified using a BCA Protein Assay kit (Pierce™) following the manufacturer's instructions. For each sample, 15 μg total proteins were mixed with 5 × SDS loading buffer and heated at 96°C for 5 min before loading onto a 10% SDS-polyacrylamide electrophoresis (PAGE) gel containing 6 M urea. After electrophoresis, the proteins were transferred to polyvinylidene fluoride (PVDF) membranes (Bio-Rad). The membranes were then blocked by PBS with 0.1% Tween® 20 (PBST) and 5% nonfat dry milk for 1 h at room temperature with gentle shaking. Next, CRISPLD2 primary antibody (anti-CRISPLD2, Sigma, HPA030055) was added to the membranes at a 1:800 dilution in PBST for overnight incubation at 4°C. Membranes were washed twice with PBST and incubated with horseradish peroxidase (HRP)-linked secondary antibodies (Sigma) at 1:100000 for 2 h at room temperature. Protein bands were detected using SuperSignal™ West Dura Extended Duration Substrate (Thermo Scientific, Rockford, IL, USA) and captured with a ChemiDoc™ Imaging System (Bio-Rad). For detection of β-Actin as a loading control, the membranes were stripped using Multi-Western™ Stripping Buffer (Bioland Scientific LLC) and re-probed with anti-Actin (Santa Cruz, sc-58673) at 1:2000 at 4°C overnight, followed by secondary antibody incubation and exposure as described above. Densitometric analysis was performed using ImageJ to quantitate the protein band intensity normalized to the control.

Collection of proteins secreted from AAV2-NULL- and AAV2-CRISPLD2-transduced hBMSCs was based on a published method with minor modifications (Mitchell et al., 2019). Briefly, cells were pelleted and washed three times with 1 × PBS. After final wash, 100 μl 1 × PBS was added to each sample without dislodging the cell pellets. After 24 h, the supernatants were filtered through 0.22 μm filter to remove any cells. The filtered supernatants containing secreted proteins were then proceeded for electrophoresis and western blot, as aforementioned, to reveal secreted CRISPLD2. The cell pellets were lysed with a cell lysis buffer to obtain the whole cell lysates and processed accordingly for western blot to detect the non-secretory CRISPLD2.

To detect matrix metallopeptidase 1 (MMP1) and forkhead box Q1 (FOXQ1) in CRISPLD2 knockdown hBMSCs, RIPA buffer (150 mM NaCl, 50 mM Tris-HCl, 1% NP-40, 0.5% sodium deoxycholate, 0.1% SDS) was used to isolate total proteins from cells.15 μg proteins were separated by 10% SDS-PAGE and transferred to a PVDF membrane. Primary antibodies, anti-MMP1 (1:800, Proteintech, 10371–2-AP) and anti-FOXQ1 (1:800, Proteintech, 23718–1-AP) were then applied to detect the target proteins as described earlier.

RNA sequencing (RNA-seq)

Total RNA was extracted from early and late passage hMSCs as previously described. The RNA concentration and OD260/280 ratio were measured by a nanodrop spectrophotometer (ThermoFisher Scientific). The RNAs with OD260/280 around 1.9 were then subjected to

electrophoresis on a 1% Clorox® denaturing agarose gel (Aranda et al., 2012). The high integrity RNAs with clear 18S and 28S rRNA bands were then sent to Arraystar Inc. (Rockville, MD, USA) for sequencing using Illumina HiSeq 4000. In comparison to the early passage, the downregulated differentially expressed genes (DEGs) in the late passage hMSCs were identified as log2FoldChange < −0.585, $p \leq 0.05$ provided by Arraystar Inc.

To investigate the effect of CRISPLD2 knockdown on the transcriptome profiling, the total RNA of hBMSCs transfected with siNC and siCRISPLD2 was extracted on day 5 post-transfection and processed as described above. The RNA samples were sent to Genewiz (South Plainfield, NJ, USA) for sequencing. The genes with |log2FoldChange| > 1, adjusted p value < 0.05 were considered as DEGs upon CRISPLD2 knockdown.

Statistical analysis

All data were presented as means ± standard deviation (SD) from at least three experiments. Two-tailed unpaired Student's t-test was used for two-group comparison, whereas one-way or two-way ANOVA followed by Tukey's test was used for pairwise comparisons among multiple groups. Differences were statistically significant when $p < 0.05$.

Results

hBMSCs, hDPSCs, and hASCs exhibit impaired osteogenic differentiation with continued in vitro expansion

To test the osteogenic differentiation potential of hMSCs during *in vitro* expansion, three different types of hMSCs, i.e., hBMSCs, hDPSCs, and hASCs, were cultured *in vitro* to passages 3, 5, 9, and 11 (P3, P5, P9, and P11). Subsequently, these hMSCs at different passages were subjected to osteogenic induction for two weeks, followed by ARS staining to demonstrate calcium deposition. As the representative staining shown in Figure 1, P3 cells possessed strong osteogenic differentiation potential, and a decrease of the potential was seen as the progress of the cell passages in all three types of hMSCs. For hBMSCs, this potential significantly decreased or even completely lost in some cases from P5. hASCs also progressively decreased osteogenic differentiation starting from P5 but to a lesser extent. Such decrease was mitigated in hDPSCs, which did not dramatically lose calcium deposition until P11.

The expression of MSC-specific surface markers remains unaltered in different passages of hBMSCs, hDPSCs, and hASCs

FACS indicated that the majority of cells in hBMSCs, hDPSCs, and hASCs of passages 3 to 11 were double positive for typical MSC surface markers (CD90, CD105) without a noticeable difference across all passages examined (Figure 2), suggesting that *in vitro* expansion did not result in the shift of subpopulations in the hMSCs. Very few double negative cells (less than 0.2%) were detected in any of the three hMSCs, indicating no overgrowth of non-hMSCs during the expansion of these hMSCs. Thus, the progressive decline of osteogenic differentiation of these three hMSCs upon continued *in vitro* expansion is not caused by the overgrowth of non-hMSCs in the population but likely is caused by intrinsic regulatory changes in the cells.

CRISPLD2 is downregulated during in vitro expansion of hBMSCs, hDPSCs, and hASCs

To understand the underlying mechanisms of loss of osteogenic differentiation in hMSCs during *in vitro* culture, RNA-seq was carried out to compare the transcriptome profiling between early and late passage hBMSCs, hDPSCs, and hASCs. A Venn diagram presented the number of downregulated genes in all these three hMSCs after *in vitro* expansion (Figure 3a). 25 downregulated genes were shared by late passage hBMSCs, hDPSCs, and hASCs. Of them, CRISPLD2 captured our attention because 1) CRISPLD2 was overall the most downregulated gene in late passage hMSCs (Figure 3b); 2) Published studies indicate that CRISPLD2 is an important protein in tissue development as homozygous CRISPLD2 knockout mice are embryonically lethal (Lan et al., 2009). Thus, we hypothesized that the expression of CRISPLD2 is critical for hMSCs to maintain their osteogenic differentiation potential when expanded *in vitro*. To test our hypothesis, we first confirmed the expression level of CRISPLD2 in hBMSCs, hDPSCs, and hASCs during their *in vitro* expansion. Compared to the early passage, the mRNA level of CRISPLD2 was remarkably decreased in late passage cells (Figure 3c). Western blot analysis showed that both secreted and non-secreted forms of CRISPLD2 proteins were reduced considerably as the passage number went higher (Figure 3d). These results suggested that the downregulation of CRISPLD2 during *in vitro* expansion of hMSCs is positively correlated to the loss of osteogenic differentiation of the cells.

Knockdown of CRISPLD2 inhibits osteogenic differentiation of hBMSCs, hDPSCs, and hASCs

To confirm the function of CRISPLD2 in hMSC osteogenic differentiation, CRISPLD2 siRNA (siCRISPLD2) was transiently transfected into P3 hBMSCs to silent endogenous CRISPLD2 expression. The duration of efficient siCRISPLD2-induced silencing was determined by qRT-PCR. As illustrated in Figure 4a, 90% knockdown was achieved through days 3–5 post-transfection, and the knockdown persisted at 70% through day 14 on average. Consistently, both secreted and non-secreted CRISPLD2 proteins were markedly decreased in siCRISPLD2-transfected cells on days 3 and 5 post-transfection as assessed by western blot shown in Figure 4b. Importantly, the extracellular matrix mineralization was severely inhibited in CRISPLD2 knockdown cells as diminished calcium deposition was observed in siCRISPLD2-transfected cells after osteogenic induction determined by ARS staining and calcium quantification, and such inhibition was in a siCRISPLD2 dose-dependent manner (Figure 4c,d). Meanwhile, the expression of osteogenic markers, such as alkaline phosphatase (ALP), bone sialoprotein (BSP), and osteopontin (OPN), was dramatically attenuated in CRISPLD2 knockdown cells (Figure 4e). Likewise, CRISPLD2 knockdown also exerted an inhibitory effect on osteogenic differentiation of hDPSCs and hASCs (Figure S1). Together, these results indicated that downregulation of CRISPLD2 inhibits osteogenic differentiation of hBMSCs, hDPSCs, and hASCs.

Knockdown of CRISPLD2 downregulates MMP1 and FOXQ1 expression in hBMSCs

Next, RNA-seq was performed to determine the effect of CRISPLD2 knockdown on transcriptome profiling. 466 statistically significant DEGs were identified in CRISPLD2 knockdown hBMSCs with $|\log2FoldChange| > 1$ and adjusted p value < 0.05 as cut-off

criteria. Of them, 191 were upregulated, and 275 were downregulated (Figure 5a). MMP1 and FOXQ1, which were reported as pro-osteogenic regulators (Wu et al., 2020; Xiang et al., 2020), were among the top ten downregulated DEGs (Figure 5b). qRT-PCR and western blot demonstrated that both mRNA and protein levels of MMP1 and FOXQ1 were significantly diminished in hBMSCs after CRISPLD2 knockdown (Figure 5c,d), suggesting that downregulation of MMP1 and FOXQ1 may contribute to CRISPLD2 knockdown-mediated impaired osteogenesis.

AAV-mediated CRISPLD2 overexpression attenuates impaired osteogenic differentiation of hBMSCs during in vitro expansion

To explore whether CRISPLD2 has a pro-osteogenic effect during *in vitro* expansion of hBMSCs, we first transduced AAV2 particles encoding CRISPLD2 (AAV2-CRISPLD2) into P9 hBMSCs at a MOI ranging from 2K to 40K to identify the optimal viral dosage. AAV2 particles without CRISPLD2 (AAV2-NULL) were used as the negative control. qRT-PCR indicated that on day 3 post-transduction, the transgenic expression of CRISPLD2 was elevated in an AAV dose-dependent manner; however, on day 7 post-transduction, CRISPLD2 reached its maximum expression at an MOI of 20K (Figure 6a). We then collected whole cell lysates and total secreted proteins at this time point for western blot analysis. As shown in Figure 6b, CRISPLD2 proteins were notably increased both in whole cell lysates and in total secreted proteins. Therefore, MOI of 20K AAV was used for overexpressing CRISPLD2 in the following experiments.

Passages 3 to 11 (P3 to P11) of hBMSCs derived from two donors were transduced with AAV2-CRISPLD2 or AAV2-NULL (control) and then subjected to osteogenic induction for three weeks to determine the effect of CRISPLD2 overexpression on the cells' osteogenic differentiation. ARS staining shown in Figure 6c indicated that CRISPLD2 overexpression could somewhat retard the loss of osteogenic differentiation in hBMSCs derived from both donors during *in vitro* expansion, although some donor-dependent variations were revealed. Specifically, for hBMSCs from Donor 1, CRISPLD2 overexpression did not show a notable difference for P3 hBMSCs compared to the control cells (AAV2-NULL transduced). However, the overexpression of CRISPLD2 could moderately recover the impaired osteogenic potential in P5 cells (Figure 6c). For hBMSCs from Donor 2, CRISPLD2 overexpression could considerably enhance the osteogenic differentiation of hBMSCs of P3 and P5 compared to the control cells transduced with AAV2-NULL (Figure 6c). Such rescuing effect of CRISPLD2 overexpression was limited for P7 hBMSCs (Figure 6c). Occasionally, we observed restoration of osteogenic differentiation in P9 and P11 hBMSCs of Donor 2 when overexpressing CRISPLD2 (Data not shown). Together, these results showed that CRISPLD2 has a pro-osteogenic effect to some extent during *in vitro* expansion of hBMSCs.

Discussion

Bone is the second most common transplanted tissue worldwide (Campana et al., 2014; W. Wang & Yeung, 2017). The osteogenic differentiation potential of hMSCs makes them promising cell sources for bone tissue engineering and regeneration (Riester et

al., 2020). *In vitro* expansion is a prerequisite for hMSCs-based therapies due to the limited availability of the primary cells (Kureel et al., 2019; Musiał-Wysocka et al., 2019; Ren et al., 2012; Wexler et al., 2003). However, hMSCs quickly lose their osteogenic differentiation potential during *in vitro* expansion, which is a major challenge in the clinical applications of hMSCs. A substantial body of research indicates that hMSCs exhibit compromised osteogenic differentiation at early passage when cultured *in vitro*; some even show attenuated osteogenesis as early as passages 1–2 which subsequently results in poor therapeutic effects *in vivo* (Chen et al., 2005; Gu et al., 2016; Siddappa et al., 2007; Yang et al., 2018). We also demonstrated that the osteogenic differentiation potential of hBMSCs, hDPSCs, and hASCs is significantly reduced during *in vitro* expansion.

It is well-known that MSCs are characterized by positive CD73, CD90, and CD105 cell surface markers, and the MSC population comprises heterogeneous cells, including non-stem cells. We conducted FACS to assess the changes in cell subpopulations during *in vitro* expansion of hMSCs (Figure 2). The result showed that hBMSCs, hDPSCs, and hASCs contain small portions of cells negative for CD90 and/or CD105, which are considered non-stem cell populations according to the abovementioned MSC characterization. Importantly, the FACS results indicated that these portions of non-stem cells did not change noticeably during expansion. Our data support the notion that cell surface marker expression is not indicative of the differentiation state of cells or their potency. For example, in passage 11, hBMSCs have completely lost osteogenic differentiation potential; however, the majority of the cells were still CD90 and CD105 positive.

Our data provided strong evidence suggesting no overgrowth of non-stem cells in the MSC population during *in vitro* expansion. Secondly, our data indicated that reduced CRISPLD2 expression contributes to the impairment of the cells' osteogenic differentiation potential during expansion. It has been reported that CRISPLD2 has the greatest fold decrease in late passage hBMSCs compared to the early passage using single-cell transcriptome sequencing (Liu et al., 2019). Our study confirmed reduced CRISPLD2 expression not only in mRNA level but also in secreted and non-secreted protein levels in hBMSCs, hDPSCs and hASCs after *in vitro* expansion. More importantly, the role of CRISPLD2 in the regulation of osteogenesis has never been explored previously. In the present study, we found that the knockdown of CRISPLD2 in early passage hMSCs abolishes the cells' osteogenic differentiation potential. The osteogenic potential diminished during *in vitro* expansion of hBMSCs could be rescued by AAV-mediated CRISPLD2 overexpression. Thus, our study, for the first time, presents evidence to reveal that CRISPLD2 is a vital regulator in maintaining osteogenic differentiation of hMSCs during *in vitro* expansion.

CRISPLD2 is considered to maturate intracellularly, followed by secretion via Golgi apparatus and ER in a process dependent on its conserved N-terminal secretory signal peptide (Oyewumi et al., 2003b). Our western blot analysis showed two immunoreactive CRISPLD2 bands in the whole cell lysates of hMSCs at different passages (Figure 3d), as well as in CRISPLD2 knockdown and overexpressing hBMSCs (Figure 4b and Figure 6b). The upper band has a molecular weight of ~56 kDa, and the lower is ~53 kDa. We collected total secreted proteins from both AAV2-NULL- and AAV2-CRISPLD2-transduced hBMSCs followed by western blot analysis. Only the lower (~53 kDa) band was shown after

immunodetection, suggesting the ~56 kDa band is the non-secreted form of CRISPLD2, whereas the ~53 kDa band is secreted form (Figure 6b). A similar pattern of CRISPLD2 protein has also been observed by Yoo et al. during *in vitro* decidualization of human endometrial stromal cells (Yoo et al., 2014).

Our data showed that hBMSCs isolated from different donors responded differently to CRISPLD2 overexpression regarding its effect on enhancing and rescuing osteogenic differentiation. For example, CRISPLD2 overexpression could considerably enhance osteogenic differentiation of P3 to P5 hBMSCs from Donor 2. However, such effect was shown mainly in P5 hBMSCs from Donor 1 (Figure 6c). Similar donor-to-donor discrepancies of specific treatment for osteogenic differentiation has also been reported in many other published studies (Franco et al., 2022; Kim et al., 2012); this could be due to donor age, health condition, and genetic backgrounds, etc. (T. Wang et al., 2020; Wilson et al., 2019). It is noteworthy that CRISPLD2 overexpression failed to rescue the impaired osteogenic potential of the P9 and P11 hBMSCs. The possible reason is that offsetting only CRISPLD2 in late passage cells is insufficient to rescue the osteogenic differentiation visibly because our RNA-seq result revealed that multiple genes are dysregulated during *in vitro* expansion of hMSCs. For instance, of the 25 downregulated genes shared by late passage hBMSCs, hDPSCs and hASCs, at least five genes have been reported as pro-osteogenic regulators, including ITGB3 (Moon et al., 2018; Yuh et al., 2020), HES4 (Cakouros et al., 2015), IRX3 (Cain et al., 2016; Tan et al., 2020), TMEM119 (Hisa et al., 2011; Tanaka et al., 2014), and TNS3 (Park et al., 2019). The downregulation of all these pro-osteogenic genes in late passage hMSCs explains why overexpressing CRISPLD2 alone in late passage cells cannot significantly restore osteogenic potential. We are currently attempting to identify the master regulatory genes causing loss of differentiation during *in vitro* expansion of hMSCs.

MMP1 and FOXQ1 are among the top ten most downregulated genes upon CRISPLD2 knockdown in hBMSCs. MMP1 is a member of the MMPs family, which degrades interstitial collagen types I, II, and III. Studies regarding its role in osteogenesis lead to contradictory findings. It has been reported that MMP1 is negatively associated with the expression of osteogenic markers and osteogenic induction (Hayami et al., 2011; Shaik et al., 2019). However, MMP1 could also serve as a pro-osteogenic factor to reverse suppressed osteogenic differentiation caused by microRNA let-7b (Y. Wang et al., 2018). Wu et al. recently provided direct evidence that MMP1 promotes osteogenic differentiation of hBMSCs via the JNK and ERK pathways (Wu et al., 2020). In the present study, we found a significant decrease of MMP1 in CRISPLD2 knockdown hBMSCs both on mRNA and protein levels. This finding is in parallel with a publication reporting that MMP1 is a target gene of CRISPLD2 in regulating the migration of lung mesenchymal and epithelial cells (H. Zhang et al., 2015). FOXQ1 is a member of the forkhead transcription factor family and is a well-known oncogene in various tumors (Tang et al., 2020; W. Wang et al., 2013). Its functions in hMSCs include enhancing the anti-senescence effect, cell migration, and cell proliferation (Tu et al., 2018; T. Zhang et al., 2018). Recently, FOXQ1 was substantiated to promote osteogenic differentiation via Wnt/β-catenin signaling (Xiang et al., 2020). Our results showed reduced FOXQ1 expression in CRISPLD2 knockdown hBMSCs. Collectively, CRISPLD2 knockdown-mediated impaired osteogenesis might be

partially attributed to the downregulation of MMP1 and FOXQ1. Further studies are needed to determine how CRISPLD2 regulates osteogenic differentiation.

In conclusion, this study indicates that the osteogenic differentiation capability of hMSCs is diminished or lost along with the decreased expression of CRISPLD2 during *in vitro* expansion. We demonstrate that suppression of CRISPLD2 inhibits the osteogenic differentiation of hMSCs. Meanwhile, AAV-mediated CRISPLD2 overexpression could attenuate or rescue the impaired osteogenic differentiation of hBMSCs during *in vitro* expansion. Thus, the reduced expression of CRISPLD2 may contribute to the loss of osteogenic differentiation observed during *in vitro* expansion of hMSCs. This work unravels a novel function of CRISPLD2 as an osteogenic regulator in hMSCs, which not only contributes to a more comprehensive understanding of the molecular mechanisms of loss of osteogenic differentiation of hMSCs during *in vitro* expansion but also provides a potential target for enhancing MSCs-based bone tissue engineering and regeneration.

Supplementary Material

Refer to Web version on PubMed Central for supplementary material.

Acknowledgments

This research was supported by the National Institutes of Health /National Institute of Arthritis and Musculoskeletal and Skin Diseases (NIAMS); Grant Number: 1R21AR076583–01A, and Louisiana Board of Regents; Grant Number: LEQSF (2020–21) -RD-A-12.

Data availability statement

All data generated or analyzed in this study are included in this article and its supporting information files. Further inquiries can be directed to the corresponding author.

References

Aranda PS, LaJoie DM, & Jorcyk CL (2012). Bleach gel: a simple agarose gel for analyzing RNA quality. Electrophoresis, 33(2), 366–369. 10.1002/elps.201100335 [PubMed: 22222980]

Aurnhammer C, Haase M, Muether N, Hausl M, Rauschhuber C, Huber I, Nitschko H, Busch U, Sing A, & Ehrhardt A (2012). Universal real-time PCR for the detection and quantification of adeno-associated virus serotype 2-derived inverted terminal repeat sequences. Human Gene Therapy, Part B: Methods, 23(1), 18–28. 10.1089/hgtb.2011.034 [PubMed: 22428977]

Bonab MM, Alimoghaddam K, Talebian F, Ghaffari SH, Ghavamzadeh A, & Nikbin B (2006). Aging of mesenchymal stem cell in vitro. BMC Cell Biology, 7, 14. 10.1186/1471-2121-7-14 [PubMed: 16529651]

Brachtl G, Poupardin R, Hochmann S, Raninger A, Jurchott K, Streitz M, Schlickeiser S, Oeller M, Wolf M, Schallmoser K, Volk HD, Geissler S, & Strunk D (2022). Batch Effects during Human Bone Marrow Stromal Cell Propagation Prevail Donor Variation and Culture Duration: Impact on Genotype, Phenotype and Function. Cells, 11(6). 10.3390/cells11060946

Cain CJ, Gaborit N, Lwin W, Barruet E, Ho S, Bonnard C, Hamamy H, Shboul M, Reversade B, & Kayserili H (2016). Loss of Iroquois homeobox transcription factors 3 and 5 in osteoblasts disrupts cranial mineralization. Bone Reports, 5, 86–95. 10.1016/j.bonr.2016.02.005 [PubMed: 27453922]

Cakouros D, Isenmann S, Hemming SE, Menicanin D, Camp E, Zannettinno ACW, & Gronthos S (2015). Novel basic helix–loop–helix transcription factor Hes4 antagonizes the function of Twist-1

to regulate lineage commitment of bone marrow stromal/stem cells. Stem Cells and Development, 24(11), 1297–1308. 10.1089/scd.2014.0471 [PubMed: 25579220]

Campana V, Milano G, Pagano E, Barba M, Cicione C, Salonna G, Lattanzi W, & Logroscino G (2014). Bone substitutes in orthopaedic surgery: from basic science to clinical practice. Journal of Materials Science: Materials in Medicine, 25(10), 2445–2461. 10.1007/s10856-014-5240-2 [PubMed: 24865980]

Chen J, Sotome S, Wang J, Orii H, Uemura T, & Shinomiya K (2005). Correlation of in vivo bone formation capability and in vitro differentiation of human bone marrow stromal cells. Journal of Medical and Dental Sciences, 52(1), 27–34. [PubMed: 15868738]

Chiquet BT, Lidral AC, Stal S, Mulliken JB, Moreno LM, Arcos-Burgos M, Valencia-Ramirez C, Blanton SH, & Hecht JT (2007). CRISPLD2: a novel NSCLP candidate gene. Human Molecular Genetics, 16(18), 2241–2248. 10.1093/hmg/ddm176 [PubMed: 17616516]

Franco RAG, McKenna E, Robey PG, Shajib MS, Crawford RW, Doran MR, & Futrega K (2022). Inhibition of BMP signaling with LDN 193189 can influence bone marrow stromal cell fate but does not prevent hypertrophy during chondrogenesis. Stem Cell Reports, 17(3), 616–632. 10.1016/j.stemcr.2022.01.016 [PubMed: 35180395]

Gaj T, & Schaffer DV (2016). Adeno-associated virus–mediated delivery of CRISPR–Cas systems for genome engineering in mammalian cells. Cold Spring Harbor Protocols, 2016(11), pdb.prot086868. 10.1101/pdb.prot086868

Gu Y, Li T, Ding Y, Sun L, Tu T, Zhu W, Hu J, & Sun X (2016). Changes in mesenchymal stem cells following long-term culture in vitro. Molecular Medicine Reports, 13(6), 5207–5215. 10.3892/mmr.2016.5169 [PubMed: 27108540]

Hayami T, Kapila YL, & Kapila S (2011). Divergent upstream osteogenic events contribute to the differential modulation of MG63 cell osteoblast differentiation by MMP-1 (collagenase-1) and MMP-13 (collagenase-3). Matrix Biology, 30(4), 281–289. 10.1016/j.matbio.2011.04.003 [PubMed: 21539914]

Hisa I, Inoue Y, Hendy GN, Canaff L, Kitazawa R, Kitazawa S, Komori T, Sugimoto T, Seino S, & Kaji H (2011). Parathyroid hormone-responsive Smad3-related factor, Tmem119, promotes osteoblast differentiation and interacts with the bone morphogenetic protein-Runx2 pathway. Journal of Biological Chemistry, 286(11), 9787–9796. 10.1074/jbc.M110.179127 [PubMed: 21239498]

Jackson RM, Griesel BA, Short KR, Sparling D, Freeman WM, & Olson AL (2019). Weight Loss Results in Increased Expression of Anti-Inflammatory Protein CRISPLD2 in Mouse Adipose Tissue. Obesity (Silver Spring), 27(12), 2025–2036. 10.1002/oby.22652 [PubMed: 31746554]

Kaplan F, Ledoux P, Kassamali FQ, Gagnon S, Post M, Koehler D, Deimling J, & Sweezey NB (1999). A novel developmentally regulated gene in lung mesenchyme: homology to a tumor-derived trypsin inhibitor. American Journal of Physiology-Lung Cellular and Molecular Physiology, 276(6), L1027–L1036. 10.1152/ajplung.1999.276.6.L1027

Kim EK, Lim S, Park JM, Seo JK, Kim JH, Kim KT, Ryu SH, & Suh PG (2012). Human mesenchymal stem cell differentiation to the osteogenic or adipogenic lineage is regulated by AMP-activated protein kinase. Journal of Cellular Physiology, 227(4), 1680–1687. 10.1002/jcp.22892 [PubMed: 21678424]

Kureel SK, Mogha P, Khadpekar A, Kumar V, Joshi R, Das S, Bellare J, & Majumder A (2019). Soft substrate maintains proliferative and adipogenic differentiation potential of human mesenchymal stem cells on long-term expansion by delaying senescence. Biology Open, 8(4). 10.1242/bio.039453

Lan J, Ribeiro L, Mandeville I, Nadeau K, Bao T, Cornejo S, Sweezey NB, & Kaplan F (2009). Inflammatory cytokines, goblet cell hyperplasia and altered lung mechanics in Lgl1+/− mice. Respiratory Research, 10, 83. 10.1186/1465-9921-10-83 [PubMed: 19772569]

Letra A, Menezes R, Cooper ME, Fonseca RF, Tropp S, Govil M, Granjeiro JM, Imoehl SR, Mansilla MA, Murray JC, Castilla EE, Orioli IM, Czeizel AE, Ma L, Chiquet BT, Hecht JT, Vieira AR, & Marazita ML (2011). CRISPLD2 variants including a C471T silent mutation may contribute to nonsyndromic cleft lip with or without cleft palate. The Cleft Palate-craniofacial Journal, 48(4), 363–370. 10.1597/09-227 [PubMed: 20815724]

Liu S, Stroncek DF, Zhao Y, Chen V, Shi R, Chen J, Ren J, Liu H, Bae HJ, Highfill SL, & Jin P (2019). Single cell sequencing reveals gene expression signatures associated with bone marrow stromal cell subpopulations and time in culture. Journal of Translational Medicine, 17(1), 23. 10.1186/s12967-018-1766-2 [PubMed: 30635013]

Mitchell R, Mellows B, Sheard J, Antonioli M, Kretz O, Chambers D, Zeuner M-T, Tomkins JE, Denecke B, & Musante L (2019). Secretome of adipose-derived mesenchymal stem cells promotes skeletal muscle regeneration through synergistic action of extracellular vesicle cargo and soluble proteins. Stem Cell Research & Therapy, 10(1), 1–19. 10.1186/s13287-019-1213-1 [PubMed: 30606242]

Moon YJ, Yun CY, Choi H, Kim JR, Park BH, & Cho ES (2018). Osterix regulates corticalization for longitudinal bone growth via integrin β3 expression. Experimental & Molecular Medicine, 50(7), 1–11. 10.1038/s12276-018-0119-9

Musiał-Wysocka A, Kot M, & Majka M (2019). The pros and cons of mesenchymal stem cell-based therapies. Cell Transplantation, 28(7), 801–812. 10.1177/0963689719837897 [PubMed: 31018669]

Nadeau K, Jankov RP, Tanswell AK, Sweezey NB, & Kaplan F (2006). Lgl1 is suppressed in oxygen toxicity animal models of bronchopulmonary dysplasia and normalizes during recovery in air. Pediatric Research, 59(3), 389–395. 10.1203/01.pdr.0000198819.81785.f1 [PubMed: 16492977]

Oyewumi L, Kaplan F, Gagnon S, & Sweezey NB (2003a). Antisense oligodeoxynucleotides decrease LGL1 mRNA and protein levels and inhibit branching morphogenesis in fetal rat lung. American Journal of Respiratory Cell and Molecular Biology, 28(2), 232–240. 10.1165/rcmb.4877 [PubMed: 12540491]

Oyewumi L, Kaplan F, & Sweezey NB (2003b). Lgl1, a mesenchymal modulator of early lung branching morphogenesis, is a secreted glycoprotein imported by late gestation lung epithelial cells. Biochemical Journal, 376(1), 61–69. 10.1042/BJ20030591 [PubMed: 12880386]

Park GC, Kim HS, Park HY, Seo Y, Kim JM, Shin SC, Kwon HK, Sung ES, Lee JC, & Lee BJ (2019). Tensin-3 regulates integrin-mediated proliferation and differentiation of tonsil-derived mesenchymal stem cells. Cells, 9(1), 89. 10.3390/cells9010089 [PubMed: 31905841]

Pittenger MF, Mackay AM, Beck SC, Jaiswal RK, Douglas R, Mosca JD, Moorman MA, Simonetti DW, Craig S, & Marshak DR (1999). Multilineage potential of adult human mesenchymal stem cells. Science, 284(5411), 143–147. 10.1126/science.284.5411.143 [PubMed: 10102814]

Quinlan J, Kaplan F, Sweezey N, & Goodyer P (2007). LGL1, a novel branching morphogen in developing kidney, is induced by retinoic acid. American Journal of Physiology-Renal Physiology, 293(4), F987–993. 10.1152/ajprenal.00098.2007 [PubMed: 17670908]

Ren G, Chen X, Dong F, Li W, Ren X, Zhang Y, & Shi Y (2012). Concise review: mesenchymal stem cells and translational medicine: emerging issues. Stem Cells Translational Medicine, 1(1), 51–58. 10.5966/sctm.2011-0019 [PubMed: 23197640]

Riester O, Borgolte M, Csuk R, & Deigner H-P (2020). Challenges in bone tissue regeneration: stem cell therapy, biofunctionality and antimicrobial properties of novel materials and its evolution. International Journal of Molecular Sciences, 22(1), 192. 10.3390/ijms22010192 [PubMed: 33375478]

Rong W, Rome C, & Yao S (2022). Increased expression of miR-7a-5p and miR-592 during expansion of rat dental pulp stem cells and their implication in osteogenic differentiation. Cells Tissues Organs, 211(1), 41–56. 10.1159/000519600 [PubMed: 34530424]

Shaik S, Martin EC, Hayes DJ, Gimble JM, & Devireddy RV (2019). Transcriptomic profiling of adipose derived stem cells undergoing osteogenesis by RNA-Seq. Scientific Reports, 9(1), 1–17. 10.1038/s41598-019-48089-1 [PubMed: 30626917]

Siddappa R, Licht R, van Blitterswijk C, & de Boer J (2007). Donor variation and loss of multipotency during in vitro expansion of human mesenchymal stem cells for bone tissue engineering. Journal of Orthopaedic Research, 25(8), 1029–1041. 10.1002/jor.20402 [PubMed: 17469183]

Swindell EC, Yuan Q, Maili LE, Tandon B, Wagner DS, & Hecht JT (2015). Crispld2 is required for neural crest cell migration and cell viability during zebrafish craniofacial development. Genesis, 53(10), 660–667. 10.1002/dvg.22897 [PubMed: 26297922]

Tan Z, Kong M, Wen S, Tsang KY, Niu B, Hartmann C, Chan D, Hui C. c., & Cheah KS (2020). IRX3 and IRX5 inhibit adipogenic differentiation of hypertrophic chondrocytes and promote osteogenesis. Journal of Bone and Mineral Research, 35(12), 2444–2457. 10.1002/jbmr.4132 [PubMed: 32662900]

Tanaka K, Kaji H, Yamaguchi T, Kanazawa I, Canaff L, Hendy GN, & Sugimoto T (2014). Involvement of the osteoinductive factors, Tmem119 and BMP-2, and the ER stress response PERK–eIF2α–ATF4 pathway in the commitment of myoblastic into osteoblastic cells. Calcified Tissue International, 94(4), 454–464. 10.1007/s00223-013-9828-1 [PubMed: 24362451]

Tang H, Zheng J, Bai X, Yue K-L, Liang J-H, Li D-Y, Wang L-P, Wang J-L, & Guo Q (2020). Forkhead box Q1 is critical to angiogenesis and macrophage recruitment of colorectal cancer. Frontiers in Oncology, 10, 564298. 10.3389/fonc.2020.564298 [PubMed: 33330033]

Tu S, Zheng J, Gao X, Guan C, Cai B, & Xiang L (2018). The role of Foxq1 in proliferation of human dental pulp stem cell. Biochemical and Biophysical Research Communications, 497(2), 543–549. 10.1016/j.bbrc.2018.02.077 [PubMed: 29453987]

Vacanti V, Kong E, Suzuki G, Sato K, Canty JM, & Lee T (2005). Phenotypic changes of adult porcine mesenchymal stem cells induced by prolonged passaging in culture. Journal of Cellular Physiology, 205(2), 194–201. 10.1002/jcp.20376 [PubMed: 15880640]

Wang T, Zhang J, Liao J, Zhang F, & Zhou G (2020). Donor genetic backgrounds contribute to the functional heterogeneity of stem cells and clinical outcomes. Stem Cells Translational Medicine, 9(12), 1495–1499. 10.1002/sctm.20-0155 [PubMed: 32830917]

Wang W, He S, Ji J, Huang J, Zhang S, & Zhang Y (2013). The prognostic significance of FOXQ1 oncogene overexpression in human hepatocellular carcinoma. Pathology-Research and Practice, 209(6), 353–358. 10.1016/j.prp.2013.03.005 [PubMed: 23623360]

Wang W, & Yeung KW (2017). Bone grafts and biomaterials substitutes for bone defect repair: A review. Bioactive Materials, 2(4), 224–247. 10.1016/j.bioactmat.2017.05.007 [PubMed: 29744432]

Wang Y, Pang X, Wu J, Jin L, Yu Y, Gobin R, & Yu J (2018). MicroRNA hsa-let-7b suppresses the odonto/osteogenic differentiation capacity of stem cells from apical papilla by targeting MMP1. Journal of Cellular Biochemistry, 119(8), 6545–6554. 10.1002/jcb.26737 [PubMed: 29384216]

Wexler SA, Donaldson C, Denning-Kendall P, Rice C, Bradley B, & Hows JM (2003). Adult bone marrow is a rich source of human mesenchymal ‘stem’cells but umbilical cord and mobilized adult blood are not. British Journal of Haematology, 121(2), 368–374. 10.1046/j.1365-2141.2003.04284.x [PubMed: 12694261]

Wilson A, Hodgson-Garms M, Frith JE, & Genever P (2019). Multiplicity of Mesenchymal Stromal Cells: Finding the Right Route to Therapy. Frontiers in Immunology, 10, 1112. 10.3389/fimmu.2019.01112 [PubMed: 31164890]

Wu Y, Tang Y, Zhang X, Chu Z, Liu Y, & Tang C (2020). MMP-1 promotes osteogenic differentiation of human bone marrow mesenchymal stem cells via the JNK and ERK pathway. The International Journal of Biochemistry & Cell Biology, 129, 105880. 10.1016/j.biocel.2020.105880 [PubMed: 33157237]

Xiang L, Zheng J, Zhang M, Ai T, & Cai B (2020). FOXQ1 promotes the osteogenic differentiation of bone mesenchymal stem cells via Wnt/beta-catenin signaling by binding with ANXA2. Stem Cell Research & Therapy, 11(1), 403. 10.1186/s13287-020-01928-9 [PubMed: 32943107]

Yang YK, Ogando CR, Wang See C, Chang TY, & Barabino GA (2018). Changes in phenotype and differentiation potential of human mesenchymal stem cells aging in vitro. Stem Cell Research & Therapy, 9(1), 131. 10.1186/s13287-018-0876-3 [PubMed: 29751774]

Yoo JY, Shin H, Kim TH, Choi WS, Ferguson SD, Fazleabas AT, Young SL, Lessey BA, Ha UH, & Jeong JW (2014). CRISPLD2 is a target of progesterone receptor and its expression is decreased in women with endometriosis. PLoS One, 9(6), e100481. 10.1371/journal.pone.0100481 [PubMed: 24955763]

Yuan Q, Chiquet BT, Devault L, Warman ML, Nakamura Y, Swindell EC, & Hecht JT (2012). Craniofacial abnormalities result from knock down of nonsyndromic clefting gene, crispld2, in zebrafish. Genesis, 50(12), 871–881. 10.1002/dvg.22051 [PubMed: 22887593]

Yuh DY, Maekawa T, Li X, Kajikawa T, Bdeir K, Chavakis T, & Hajishengallis G (2020). The secreted protein DEL-1 activates a β3 integrin–FAK–ERK1/2–RUNX2 pathway and promotes osteogenic differentiation and bone regeneration. Journal of Biological Chemistry, 295(21), 7261–7273. 10.1074/jbc.RA120.013024 [PubMed: 32280065]

Zhang H, Sweezey NB, & Kaplan F (2015). LGL1 modulates proliferation, apoptosis, and migration of human fetal lung fibroblasts. American Journal of Physiology-Lung Cellular and Molecular Physiology, 308(4), L391–402. 10.1152/ajplung.00119.2014 [PubMed: 25480331]

Zhang T, Wang P, Liu Y, Zhou J, Shi Z, Cheng K, Huang T, Wang X, Yang GL, & Yang B (2018). Overexpression of FOXQ1 enhances anti-senescence and migration effects of human umbilical cord mesenchymal stem cells in vitro and in vivo. Cell and Tissue Research, 373(2), 379–393. 10.1007/s00441-018-2815-0 [PubMed: 29500491]

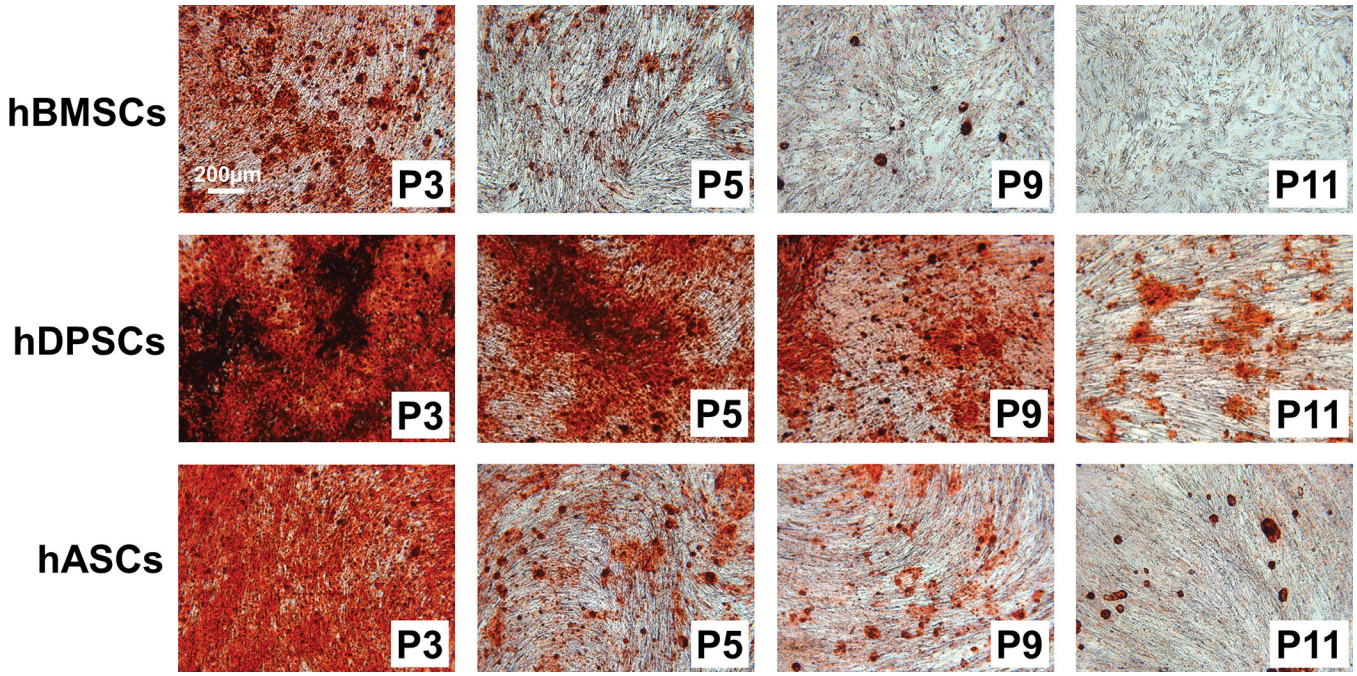

Figure 1.

hBMSCs, hDPSCs, and hASCs exhibit impaired osteogenic differentiation with continued *in vitro* expansion. ARS staining shows markedly diminished calcium nodules in late passage compared to early passage cells. Note the intense ARS staining in passage 3 (P3) for all cells and reduced staining as the increase of the passages from passage 5 (P5) to passage 11 (P11). However, hBMSCs appear to reduce the staining quickest among the three hMSCs.

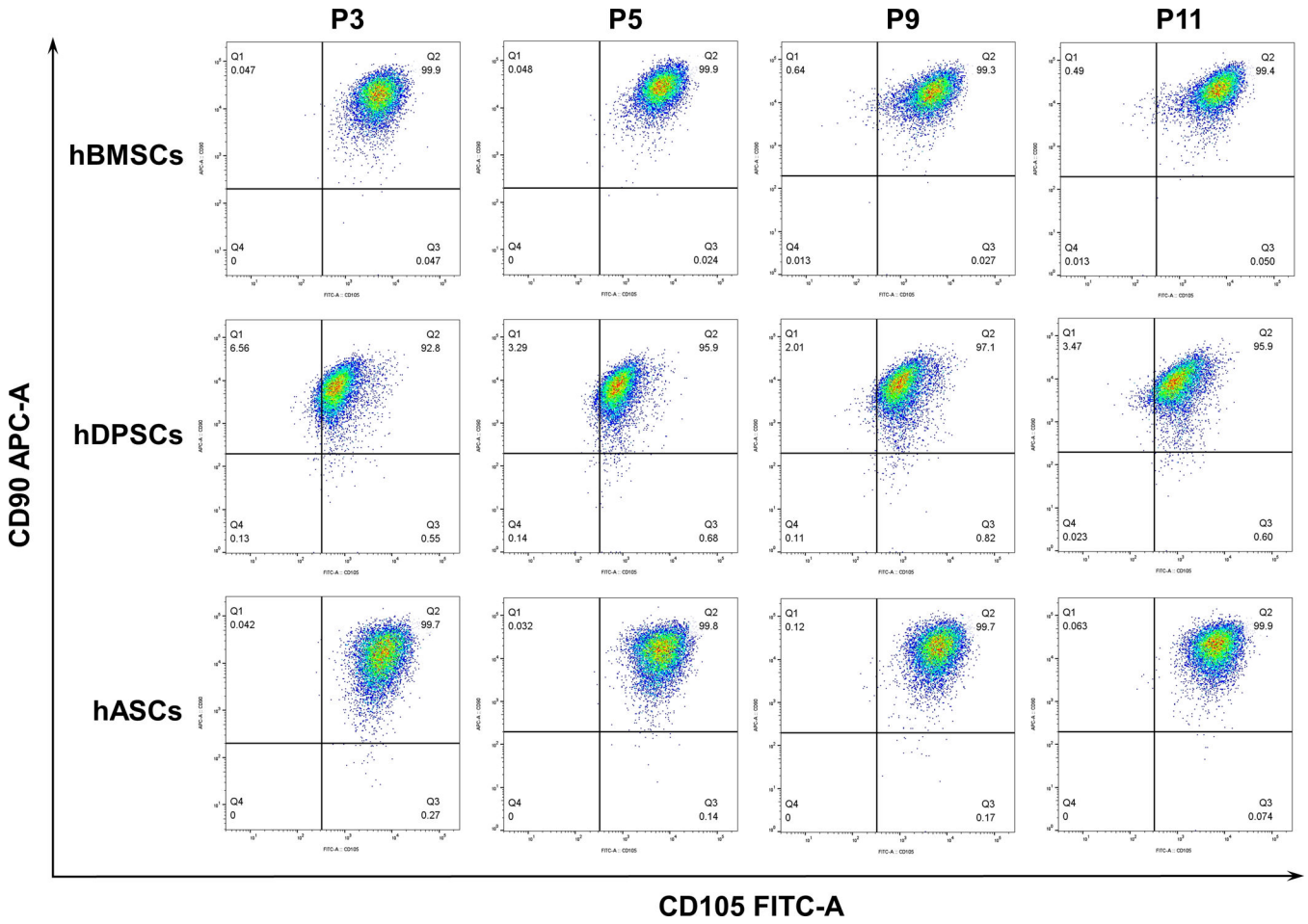

Figure 2.

The expression of MSC-specific surface markers, CD90 and CD105, remains unaltered in different passages of hBMSCs, hDPSCs, and hASCs. FACS indicates no remarkable changes of CD90 and CD105 expression in passages (P) 3, 5, 9, and 11. Please noted that over 99% of hBMSCs and hASCs were found to be double positive for the CD90 and CD105 markers, and more than 92% of hDPSCs were double positive for CD90 and CD105 across all passages examined. Very few double negative (less than 0.2%) cells were detected in any of the three hMSCs.

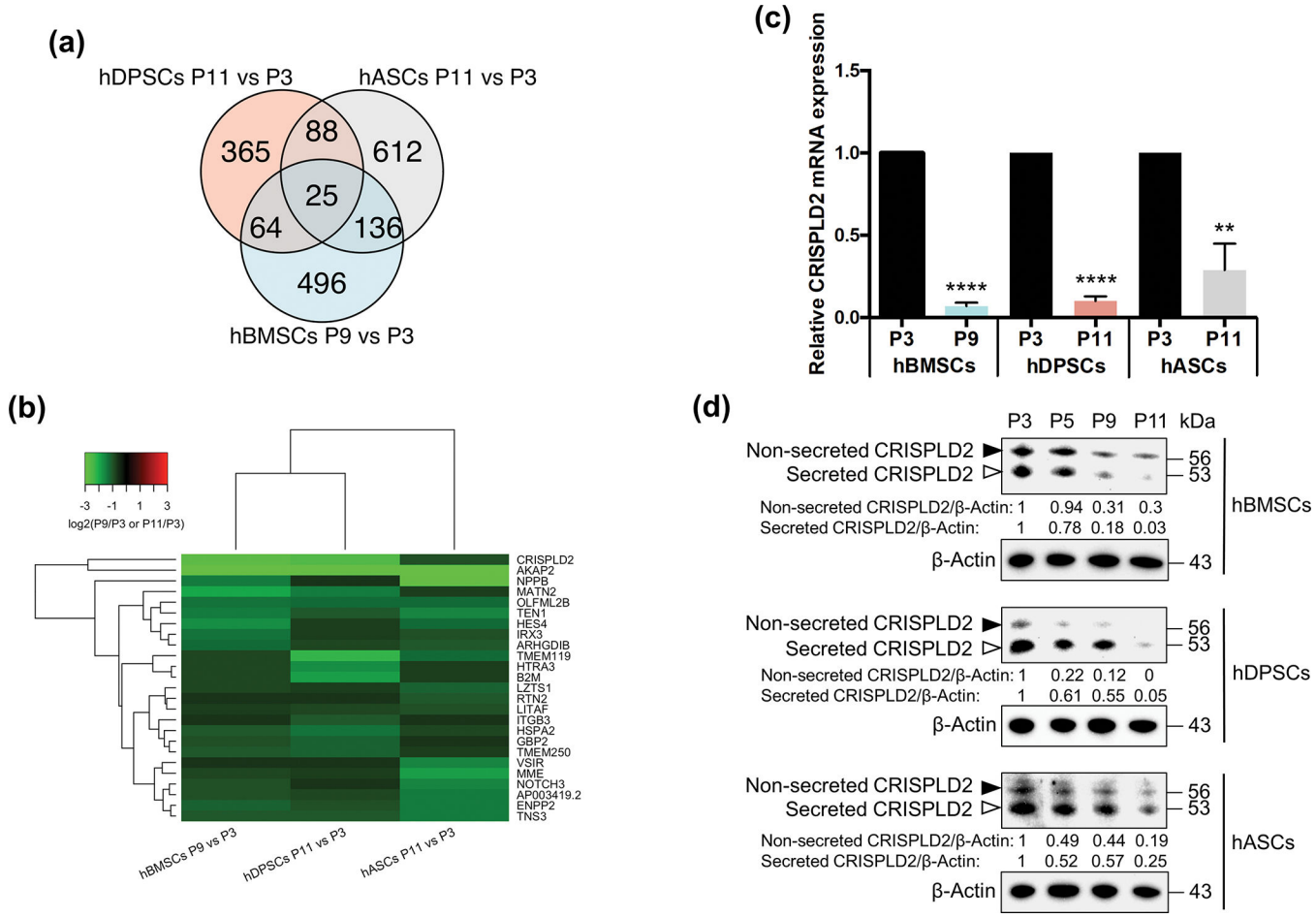

Figure 3.

CRISPLD2 is downregulated during *in vitro* expansion of hBMSCs, hDPSCs, and hASCs. (a) Venn diagram generated from RNA-seq data shows the number of significantly downregulated genes in late passage hMSCs (hBMSCs, hDPSCs, and hASCs) with log2FoldChange < −0.585, $p \leq 0.05$. (b) Heatmap presents the 25 downregulated genes shared by late passage hBMSCs, hDPSCs, and hASCs. (c) Relative mRNA level of CRISPLD2 in early and late passage hBMSCs, hDPSCs, and hASCs, as determined by qRT-PCR. Data are presented as means ± SD (n = 3). $^{**}p < 0.01$, $^{****}p < 0.0001$ with Student's *t*-test. (d) The protein level of CRISPLD2 in hBMSCs, hDPSCs, and hASCs at different passages detected by western blot. Densitometric analysis of CRISPLD2 levels normalized to β-Actin was shown below immunoblot bands. Black arrows indicate the non-secreted form of CRISPLD2 protein; white arrows denote the secreted form of CRISPLD2 protein. Note the reduction of CRISPLD2 protein as the increase of the cell passages from passage 3 (P3) to passage 11 (P11).

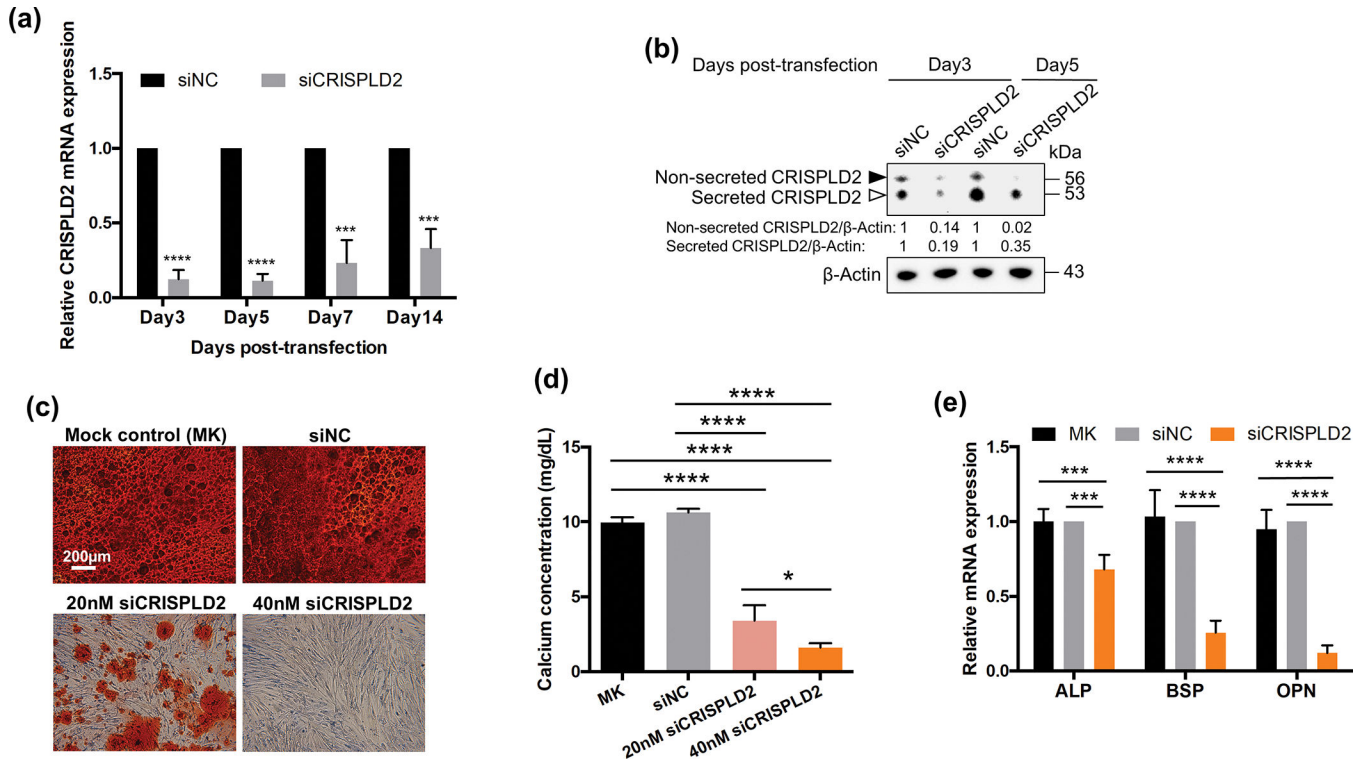

Figure 4.

Knockdown of CRISPLD2 inhibits osteogenic differentiation of hBMSCs in a siRNA dose-dependent manner. CRISPLD2 knockdown efficiency was assessed by qRT-PCR (a) and western blot (b) on different days after siRNA transfection showing successful knockdown of CRISPLD2. ***$p < 0.001$, ****$p < 0.0001$ with Student's *t*-test. Densitometric analysis of CRISPLD2 levels normalized to β-Actin was shown below immunoblot bands. The black arrow indicates the non-secreted form of CRISPLD2 protein; the white arrow denotes the secreted form of CRISPLD2 protein. (c) ARS staining and (d) quantification of the calcium deposition in hBMSCs transfected with siRNA concentrations of 20 nM and 40 nM, indicating that siCRISPLD2 suppresses osteogenic differentiation in a dose-dependent manner. *$p < 0.05$, ****$p < 0.0001$ with one-way ANOVA followed by Tukey's test. (e) Relative mRNA levels of osteogenic markers ALP, BSP, and OPN in hBMSCs upon CRISPLD2 knockdown were determined by qRT-PCR after three weeks of osteo-induction. ***$p < 0.001$, ****$p < 0.0001$ with two-way ANOVA followed by Tukey's test. All data are presented as means ± SD (n = 3).

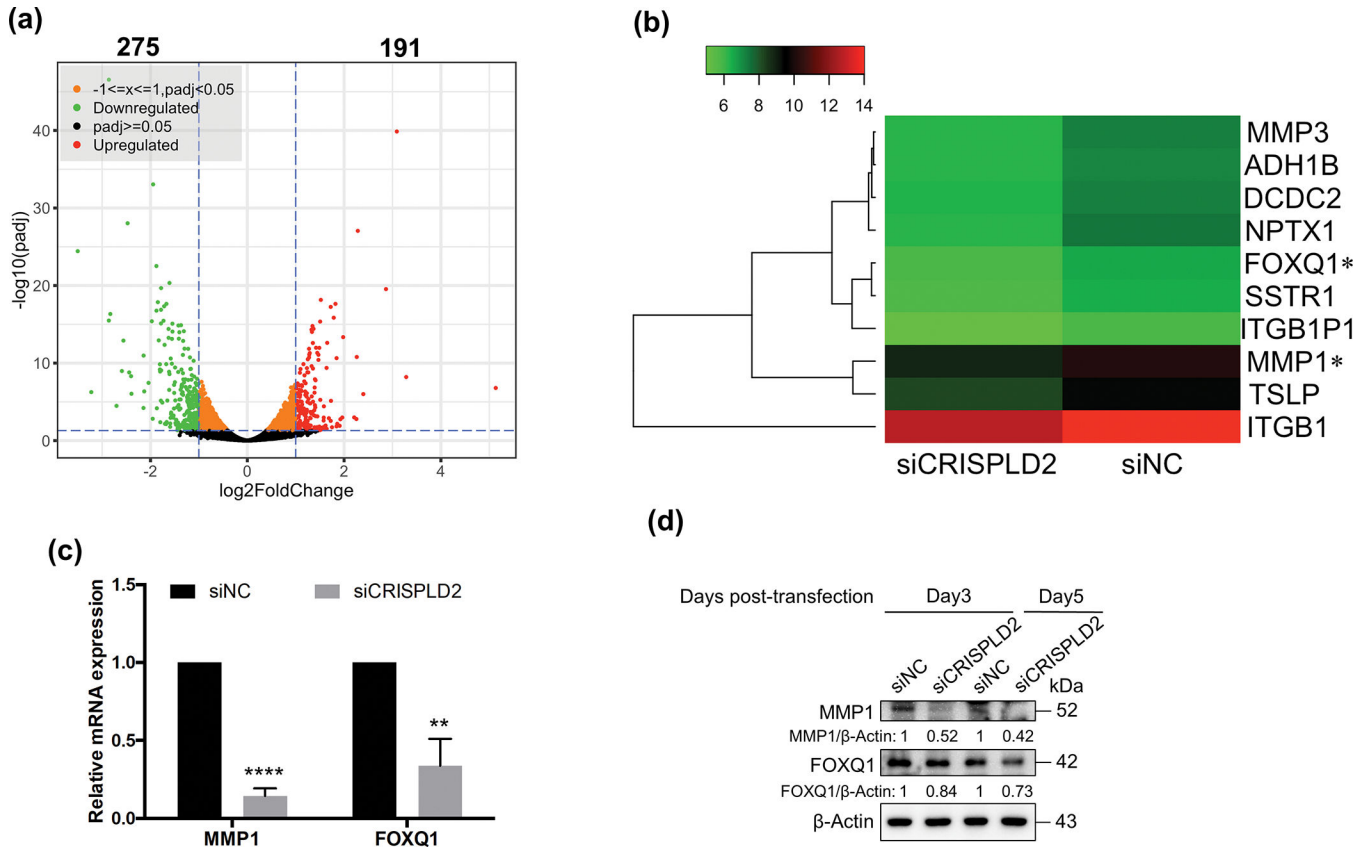

Figure 5.

Knockdown of CRISPLD2 downregulates MMP1 and FOXQ1 expression in hBMSCs. (a) Volcano plot shows transcriptome changes in hBMSCs upon CRISPLD2 knockdown. Green and red dots represent significantly downregulated and upregulated DEGs, respectively. The genes with |log2FoldChange| > 1, adjusted *p* value (padj) < 0.05 are defined as significant DEGs. Black dots represent unaltered genes (padj ≥ 0.05). Orange dots represent DEGs with |log2FoldChange| ≤ 1 and padj < 0.05. Dashed lines denote the significance threshold. (b) Heatmap demonstrates the top ten most downregulated genes in CRISPLD2 knockdown hBMSCs. Asterisks indicate the genes with pro-osteogenic roles selected for further study. (c) Relative mRNA levels of MMP1 and FOXQ1 in siCRISPLD2-transfected hBMSCs were determined by qRT-PCR on day 5 post-transfection. Data are presented as means ± SD (n=3). $^{**}p < 0.01$, $^{****}p < 0.0001$ with Student's *t*-test. (d) Protein levels of MMP1 and FOXQ1 in CRISPLD2 knockdown hBMSCs were detected by western blot on days 3 and 5 post-transfection. Densitometric analysis of MMP1 and FOXQ1 levels normalized to β-Actin was shown below immunoblot bands.

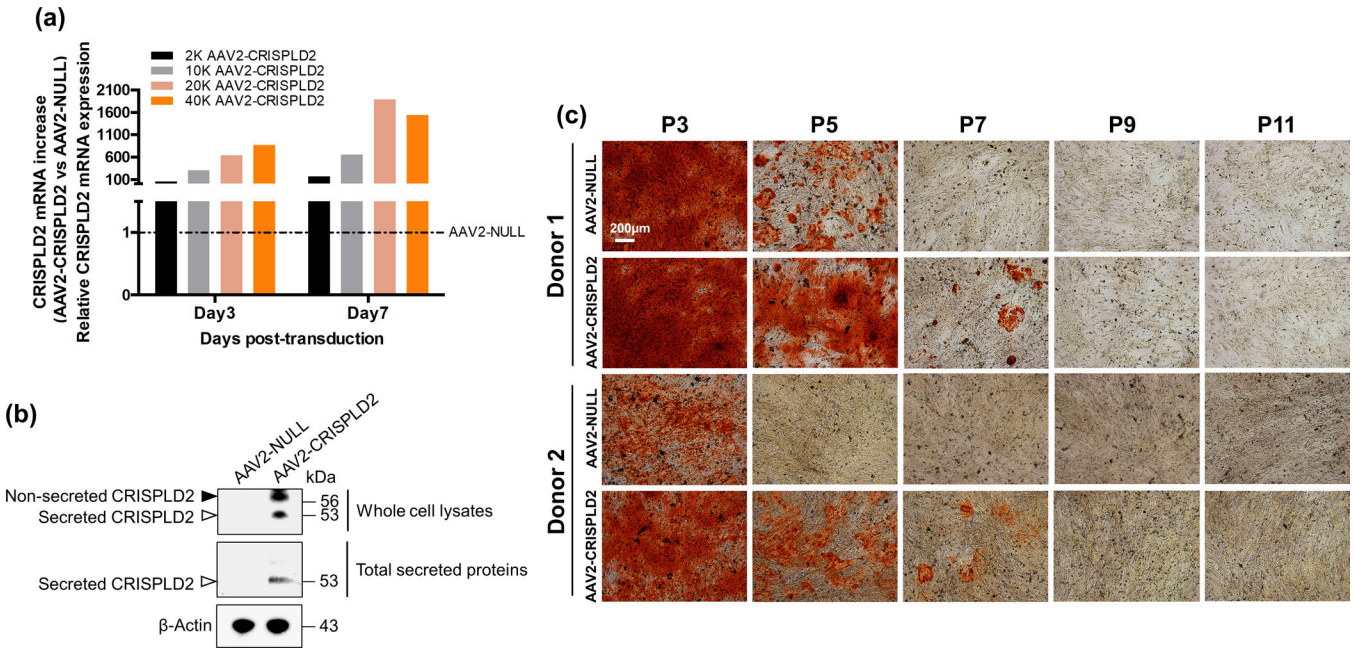

Figure 6.

AAV-mediated CRISPLD2 overexpression attenuates impaired osteogenic differentiation of hBMSCs during *in vitro* expansion. (a) Transduction of hBMSCs with AAV2-CRISPLD2 at different MOI results in CRISPLD2 mRNA increase, as measured by qRT-PCR. The dashed line represents the CRISPLD2 mRNA level in AAV2-NULL (control) transduced hBMSCs. (b) Western blot shows elevated CRISPLD2 expression in both whole cell lysates and total secreted proteins on day 7 after transduction of AAV2-CRISPLD2 at an MOI of 20K. Black arrows indicate the non-secreted form of CRISPLD2 protein (~56 kDa); white arrows denote the secreted form of CRISPLD2 protein (~53 kDa). Note that only the lower band (~53 kDa) appears in total secreted proteins. (c) Microscopic images of ARS staining showing matrix mineralization of different passages of hBMSCs from two individual donors in response to CRISPLD2 overexpression after three weeks of osteogenic induction. Note the enhanced ARS staining in P3 (hBMSCs from Donor 2 only), P5 and P7 cells transduced with AAV2-CRISPLD2 compared to the control cells transduced with AAV2-NULL.